

Preparation and characterization of a zinc oxide nanopowder supported onto inorganic clay.

Original

Preparation and characterization of a zinc oxide nanopowder supported onto inorganic clay / Hassan, Mohamed; Afify, AHMED SABRY SHEHATA; Ataalla, Mohamed; Mohammed, Amr; Staneva, Anna; Dimitriev, Yanko; Tulliani, Jean Marc Christian. - In: JOURNAL OF CHEMICAL TECHNOLOGY AND METALLURGY. - ISSN 1314-7471. - STAMPA. - 51:2(2016), pp. 168-172.

Availability:

This version is available at: 11583/2678629 since: 2017-09-04T12:41:11Z

Publisher:

University of Chemical Technology and Metallurgy

Published

DOI:

Terms of use:

This article is made available under terms and conditions as specified in the corresponding bibliographic description in the repository

Publisher copyright

(Article begins on next page)

PREPARATION AND CHARACTERIZATION OF A ZINC OXIDE NANOPOWDER SUPPORTED ONTO INORGANIC CLAY

Mohamed Hassan¹, Ahmed Sabry Afify², Mohamed Ataalla^{3,4}, Amr Mohammed⁵,

Anna Staneva³, Yanko Dimitriev³, Jean-Marc Tulliani²

¹ Department of Natural Science
Obour Institute of Engineering and Technology
Obour, Egypt

Received 28 November 2015

Accepted 05 February 2016

² Politecnico di Torino
Department of Applied Science and Technology
10129 Torino, Italy

³ University of Chemical Technology and Metallurgy
8 Kl. Ohridski, 1756 Sofia, Bulgaria
E-mail: sobhy.88@hotmail.com

⁴ Department of Chemical Engineering,
Faculty of Engineering,
Badr University in Cairo (BUC), Egypt

⁵ Chemistry Department, Deanery of Academic Services
Taibah University, Al-Madinah Al-Munawwarah
Saudi Arabia
On a sabbatical leave from the Higher
Institute of Optics Technology, Heliopolis, Cairo, Egypt

ABSTRACT

Zinc oxide nanoparticles are obtained by a wet chemical method using zinc sulphate as a raw material. Doping sepiolite, micro-fibrous inorganic clay, with ZnO after precipitation under basic conditions and subsequent thermal treatment is investigated as both materials are abundant. They are used for the development of humidity and gas sensors of great environmental importance.

The particle size distribution, the morphology and the composition of the powder samples are characterized by X-Ray diffraction accompanied by Field Emission Scanning Electron Microscopy and High Resolution-Transmission Electron Microscopy techniques. The data obtained confirm the formation of zinc oxide nanoparticles of a size of 10 nm on the modified sepiolite grains.

Keywords: ZnO, sepiolite, nanoparticles, doping.

INTRODUCTION

Zinc oxide is a semiconductor with a wide band gap of 3.37 eV at room temperature [1]. It has been thoroughly investigated because of its unique physical and chemical properties which make it an excellent material for electronic [2], piezoelectric [3] and optical devices [4] as well as gas sensors [5].

The inherent properties of nanometal oxides of different structures, the gas-sensing property [6, 7] in

particular, have been investigated. Various methods have been developed for ZnO nanopowders preparation [8] including the soft chemical method [9], the sol-gel process [10], the vapor phase growth [11], the vapor-liquid-solid process [12], etc. The choice of a suitable precursor for the synthesis of a ZnO nano-crystal affects its purity, morphology, size and thus, plays a crucial role in determining the properties provided by the resultant applications.

Sepiolite is micro-fibrous inorganic clay whose

chemical formula is $\text{Mg}_8\text{Si}_{12}\text{O}_{30}(\text{OH})_4(\text{H}_2\text{O})_4 \cdot 8\text{H}_2\text{O}$. Its structural units are composed of two tetrahedral silica sheets and a discontinuous central layer of an octahedral magnesium oxide. This gives rise to the formation of open channels of dimensions of 0.36 nm x 1.06 nm [13].

The clay doping with metal ions has been studied extensively because they as well as the metal ions are abundant materials. Besides, useful applications of environmental importance [14 - 16] can be engineered such as those referring to the development of gas and humidity sensors.

This paper describes the preparation of ZnO nanocrystals by chemical synthesis using zinc sulphate and sepiolite as raw materials. It reports their characterization by means of laser granulometry, X-ray diffraction (XRD), Field Emission Scanning Electron Microscopy (FESEM) and High Resolution Transmission Electron Microscopy (HRTEM).

EXPERIMENTAL

Materials Preparation

All the reagents were ACS grade supplied from Sigma-Aldrich. The natural sepiolite, a product of Vicalvaro-Vallecas (TOLSA, PangelS9, Spain) was dispersed in distilled water to reach 10 mass % concentration. Then, the suspension was progressively acidified at a room temperature with 37 % HCl at pH = 0 for 2 h. The dispersion obtained was vacuum filtered and subsequently washed with distilled water (2 - 3 times). After that, the sample was mixed with 1.0 L of an aqueous solution of $\text{ZnSO}_4 \cdot \text{H}_2\text{O}$ and the pH of the dispersion was adjusted with sodium hydroxide to (pH = 9) to ensure the precipitation of all zinc ion species. Finally, the dispersion obtained was dried overnight at 150°C and subsequently calcinated at 550°C for 1 h at a heating rate of 2°C/min.

Material characterization

The particle size distribution was determined after powders calcination followed by dispersion in ethanol and sonication for 10 min. A laser granulometer (Malvern 3600D, Great Britain) was used.

The X-ray diffraction patterns of calcined powder samples were collected by X'PertHighScore Philips Analytical Diffractometer equipped with a Cu anticathode (λ Cu $K\alpha$ anticathode = 0.154056 nm). The samples

were scanned at a rate of 0.02°/s in the range from 5° to 70° in 2θ .

The morphology of the powders was inspected by Field Emission Scanning Electron Microscopy (FE-SEM, Zeiss Merlin) and High Resolution-Electron Transmission Microscopy (HR-TEM) using a JEOL 3010-UHR instrument (acceleration potential: 300 kV; LaB_6 filament), equipped with an Oxford INCA X-ray energy dispersive spectrometer (X-EDS) with a Pentafet Si(Li) detector.

RESULTS AND DISCUSSION

Particle size distribution

Table 1 shows that the zinc doped sepiolite (Zn-S) thermally treated for 1 h at 550°C has a larger particle size distribution than pure sepiolite (S). This may be attributed to the attachment force leading to particles agglomeration because of the presence of either electrostatic or Van der Waals forces or the development of material bridges through the presence of a liquid during the processes of leaching and washing of pure sepiolite [17].

X-Ray diffraction

The XRD patterns of pure sepiolite and ZnO doped sepiolite after 2 h of acid leaching and heat treatment for 1 h at 550°C are listed in Fig. 1. The XRD pattern of pure sepiolite is indexed as JCPDS card no.(13-595), while the leached heat treated sample is indexed as anhydrous sepiolite [18]. ZnO is detected in the Zn-S sample and indexed as JCPDS card no.(36-1451).

Several reflections, such as the reflection of the main

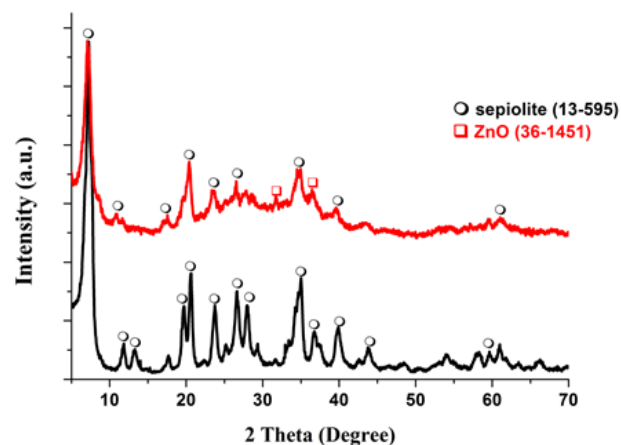


Fig. 1. XRD pattern of sepiolite and ZnO doped sepiolite.

Table 1. Cumulative distribution of pure sepiolite(S) and zinc doped sepiolite (Zn- S).

Cumulative mass %	S	Zn-S
10	3.1	4.5
50	7.1	18.8
90	19.5	74.3

peak of the pristine sepiolite that is outlined at 1.200 nm (7.36° in 2θ , (110)) or reflections at 0.757 nm (11.68° in 2θ , (130)), 0.662 nm (13.36° in 2θ , (040)) and 1.970 nm (4.48° in 2θ , (060)) disappear, whereas two new reflection peaks appear at 0.999 nm (8.84° in 2θ , (110)) and 0.795 nm (11.12° in 2θ , (120)) corresponding to the folded monoclinic structure [17]. In this case, the reflection of the main peak occurs at 0.439 nm (20.21° in 2θ , (121)) which confirms the presence of both folded and unfolded sepiolite (Fig.1).

The acid treatment of sepiolite removes Mg^{2+} located in its octahedral layer but leaves Si^{4+} coordinated in its tetrahedral one [19]. It is reported that the acid treatment of sepiolite with H_2SO_4 results in Si-O-Mg-O-Si bond transformation in two Si-O-H bonds [20]. Thus, the internal channels interconnect, while the specific surface area increases. In case most of the magnesium ions are removed, some of the micro- and mesopores expand to macropores. It is found that the formation of an anhydrous sepiolite structure of nanosize channels, providing the coexistence of sepiolite and silica in the same fiber, is responsible for its thermal stabilization [18].

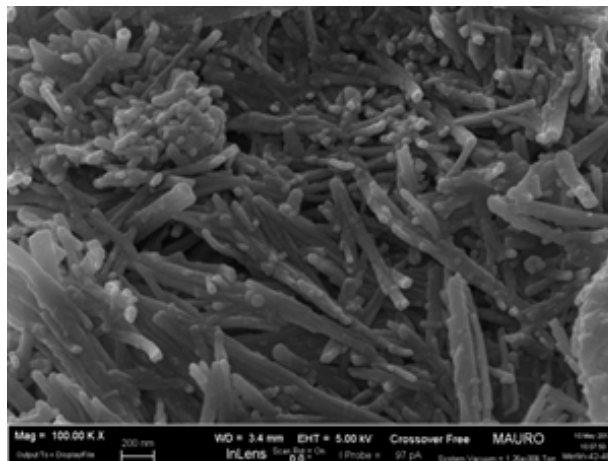
FE-SEM observation

The surface morphologies of the thermally treated sepiolite and the zinc doped sepiolite are shown in Figs. 2a, 2b and 2c, correspondingly. They are observed by FESEM. It is evident that there is no significant difference between the samples prior to and after the leaching, the sepiolite precipitation and the thermal treatment. This is in agreement with the XRD data.

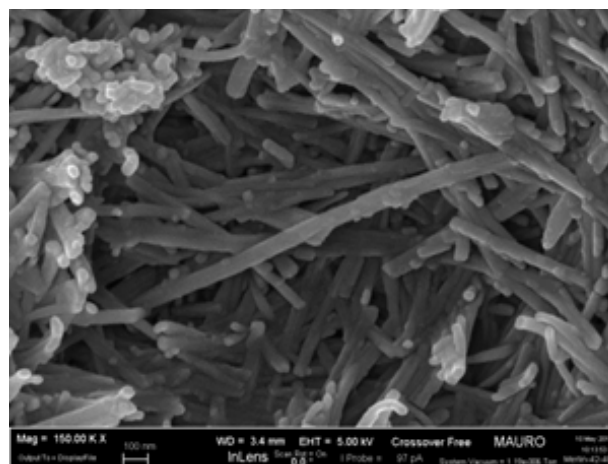
Table 2. EDX analysis of ZnO doped sepiolite sample.

Metals	Mass %
Mg	24.4
Si	55.8
Zn	19.8

a)



b)



c)



Fig. 2. (a) micrograph of thermally treated sepiolite; (b) FE-SEM micrograph of thermally treated leached sepiolite; (c) FE-SEM micrograph of zinc doped sepiolite.

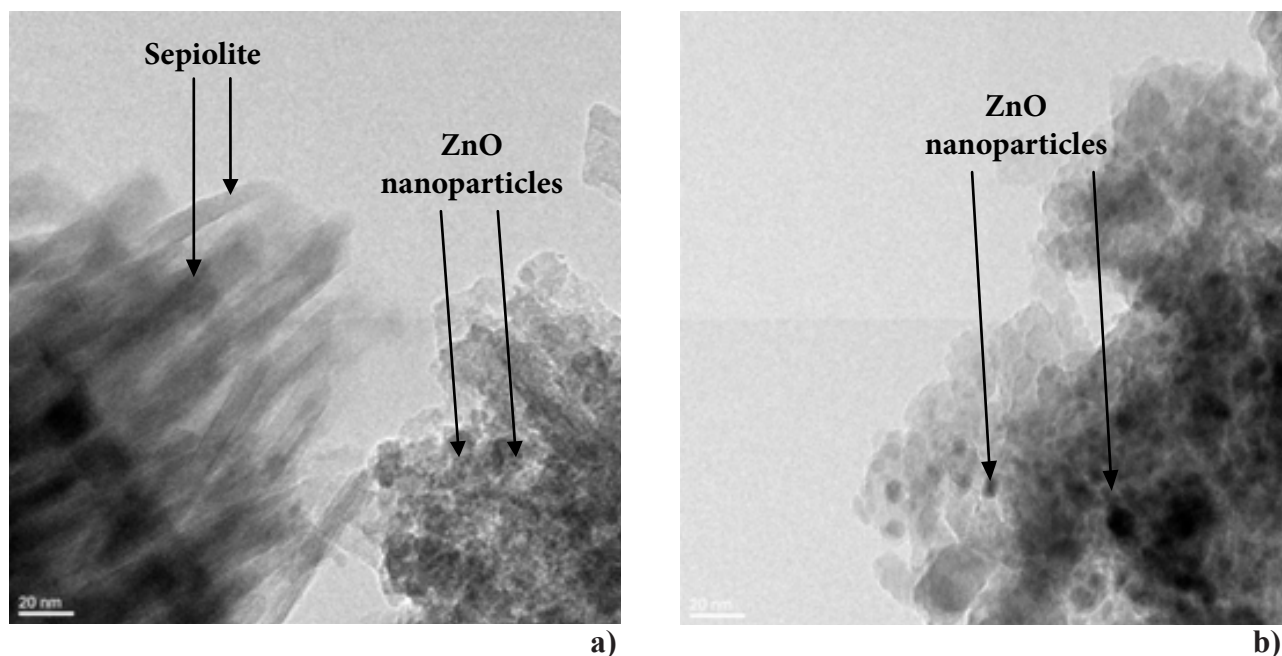


Fig. 3. HR-TEM micrographs of ZnO doped sepiolite (a) and ZnO nanoparticles (b).

Energy dispersive X-ray spectroscopy (EDX)

Semi-quantitative elemental analysis of ZnO-doped sepiolite shows that Mg^{+2} and Zn^{2+} are well distributed in the powder. Table 2 indicates a zinc content of 19.8 mass % of the sample prepared. This is an evidence of the presence of ZnO within the anhydride sepiolite.

HRTEM observation

Fig. 3a shows that the structure of sepiolite is crystalline (the atomic planes are visible in the needles of sepiolite on the left side of the micrograph). This is in agreement with the XRD data. Besides, ZnO nanoparticles are seen on the right side. Fig. 3b shows that the ZnO nanoparticles having a diameter below 10 nm are mostly located on the surface of the sepiolite grains.

CONCLUSIONS

A chemical route for the preparation of a nanopowder of ZnO precipitated onto sepiolite by using zinc sulphate was described. The results showed that nano-zinc oxide crystals grew onto the grains of the modified sepiolite. HRTEM micrographs showed that the particle size of ZnO was less than 10 nm.

The fact that nanoparticles are grown on an inert matrix provides the exclusion of additional manipulations and pure nanoparticles disadvantages. The method advanced is economically favorable in view of the large deposits of sepiolite and metal salts, the short preparation

time and the simple operations required.

REFERENCES

1. M.Z.B. Hussein, W.H.W. Azmin, M. Mustafa, A.H. Yahaya, Bacillus cereus as a biotemplating agent for the synthesis of zinc oxide with raspberry- and plate-like structures, *J. Inorg. Biochem.*, 103, 2009, 1145-1150.
2. S. Singh, P. Thiyagarajan, K.M. Kant, D. Anita, S. Thirupathiah, N. Rama, B. Tiwari, M. Kottaisamy, M.R. Rao, Structure, microstructure and physical properties of ZnO based materials in various forms: bulk, thin film and nano, *J. Phys.*, D 40, 2007, 6312-6327.
3. N.W. Emanetoglu, C. Gorla, Y. Liu, S. Liang, Y. Lu, Epitaxial ZnO piezoelectric thin films for saw filters, *Mater. Sci. Semiconduct. Process.*, 2, 1999, 247-252.
4. S.H. Jeong, B.N. Park, S.B. Lee, J.H. Boo, Structural and optical properties of silver-doped zinc oxide sputtered films, *Surf. Coat. Technol.*, 193, 2005, 340-344.
5. C.D. Lokhande, P.M. Gondkar, R.S. Mane, V.R. Shinde, S.-H. Han, CBD grown ZnO-based gas sensors and dye-sensitized solar cells, *J. Alloys Compd.*, 475, 2009, 304-311.
6. X.Y. Lai, D. Wang, N. Han, J. Du, J. Li, C.J. Xing, Y.F. Chen, X.T. Li, Ordered arrays of bead-Chain-like In_2O_3 nanorods and their enhanced sensing perfor-

- mance for formaldehyde, *Chem. Mater.*, 22, 2010, 3033-3042.
7. R.B. Yu, Z.M. Li, D. Wang, X.Y. Lai, C.J. Xing, M. Yang, X.R. Xing, $\text{Fe}_2\text{TiO}_5/\alpha\text{-Fe}_2\text{O}_3$ nanocomposite hollow spheres with enhanced gas-sensing properties, *Scr. Mater.*, 63, 2010, 155-158.
 8. A. Moezzi, A.M. McDonagh, M.B. Cortie, Zinc oxide particles: Synthesis, properties and applications, *Chem. Eng. J.*, 185-186, 2012, 1-22.
 9. L. Vayssieres, Growth of arrayed nanorods and nanowires of ZnO from aqueous solutions, *Adv. Mater.*, 15, 5, 2003, 464-466.
 10. H. Zhang, X.Y. Ma, J. Xu, J. Niu, D. Yang, Arrays of ZnO nanowires Fabricated By A Simple Chemical Solution Route, *Nanotechnology*, 14, 4, 2003, 423-426.
 11. X.C. Sun, H.Z. Zhang, J. Xu, Q. Zhao, R. M. Wang, D.P. Yu, Shape controllable synthesis of ZnO nanorod arrays via vapor phase growth, *Solid State Commun.*, 129, 12, 2004, 803-807.
 12. P.X. Gao, Z.L. Wang, Nanopropeller arrays of zinc oxide, *Appl. Phys. Lett.*, 84, 15, 2004, 2883-2885.
 13. T. Hibino, A. Tsunashima, A. Yamazaki, R. Otsuka, Model calculation of sepiolite surface areas, *Clays Clay Miner.*, 43, 4, 1995, 391-396.
 14. Z. Ding, R.L. Frost, Study of copper adsorption on montmorillonites using thermal analysis methods, *J. Colloid Interface Sci.*, 269, 2004, 296-302.
 15. A. Esteban-Cubillo, J.M. Tulliani, C. Pecharromán, J.S. Moya, Iron oxide nanoparticles supported on sepiolite as a novel humidity sensor, *J. Eur. Ceram. Soc.*, 27, 2007, 1983-1989.
 16. Ahmed S. Afify, M. Hassan, M. Piumetti, I. Peter, B. Bonelli, J.-M. Tulliani, Elaboration and characterization of modified sepiolites and their humidity sensing features for environmental monitoring, *Applied Clay Sci.*, 115, 2015, 165-173.
 17. S.J.R. Simons, R.J. Fairbrother, Direct observations of liquid binder-particle interactions: the role of wetting behaviour in agglomerate growth, *Powder Technol.*, 110, 2000, 44-58.
 18. J.L. Valentin, M.A. Lopez-Manchado, A. Rodriguez, P. Posadas, L. Ibarra, Novel anhydrous unfolded structure by heating of acid pre-treated sepiolite, *Applied Clay Sci.*, 36, 2007, 245-255.
 19. A. Miura, K. Nakazawa, T. Takei, N. Kumada, N. Kinomura, R. Ohki, H. Koshiyama, Acid- base- and heat-induced degradation behavior of Chinese sepiolite, *Ceram. Int.*, 38, 2012, 4677-4684.
 20. F. Wang, J.S. Liang, Q.G. Tang, J.P. Meng, Z.Z. Wu, G.-S. Li, Microstructure of sepiolite and its adsorbing properties to dodecanol, *Trans. Nonferrous Met. Soc. China*, 16, 2006, 406-410.